

CLINICAL STUDY



EP300-mediated H3 acetylation elevates MTHFD2 expression to reduce mitochondrial dysfunction in lipopolysaccharide-induced tubular epithelial cells

Weike Hu

Department of Emergency Medicine, The First Affiliated Hospital of Ningbo University, Ningbo, China

ABSTRACT

Sepsis represents an organ dysfunction resulting from the host's maladjusted response to infection, and can give rise to acute kidney injury (AKI), which significantly increase the morbidity and mortality of septic patients. This study strived for identifying a novel therapeutic strategy for patients with sepsis-induced AKI (SI-AKI). Rat tubular epithelial NRK-52E cells were subjected to lipopolysaccharide (LPS) exposure for induction of *in-vitro* SI-AKI. The expressions of E1A binding protein p300 (EP300) and methylenetetrahydrofolate dehydrogenase 2 (MTHFD2) in NRK-52E cells were assessed by western blot and qRT-PCR, and their interaction was explored by chromatin immunoprecipitation performed with antibody for H3K27 acetylation (H3K27ac). The effect of them on SI-AKI-associated mitochondrial dysfunction of tubular epithelial cells was investigated using transfection, MTT assay, TUNEL staining, 2',7'-Dichlorodihydrofluorescein diacetate probe assay, Mitosox assay, and JC-1 staining. MTHFD2 and EP300 were upregulated by LPS exposure in NRK-52E cells. LPS increased the acetylation of H3 histone in the MTHFD2 promoter region, and EP300 suppressed the effect of LPS. EP300 ablation inhibited the expression of MTHFD2. MTHFD2 overexpression antagonized LPS-induced viability reduction, apoptosis promotion, reactive oxygen species overproduction, and mitochondrial membrane potential collapse of NRK-52E cells. By contrast, MTHFD2 knockdown and EP300 ablation brought about opposite consequences. Furthermore, MTHFD2 overexpress and EP300 ablation counteracted each other's effect in LPS-exposed NRK-52E cells. EP300-mediated H3 acetylation elevates MTHFD2 expression to reduce mitochondrial dysfunction of tubular epithelial cells in SI-AKI.

ARTICLE HISTORY

Received 12 July 2023
Revised 4 June 2024
Accepted 12 June 2024

KEYWORDS

E1A binding protein p300; methylenetetrahydrofolate dehydrogenase 2; sepsis-induced acute kidney injury; tubular epithelial cells; mitochondrial dysfunction



Introduction

Sepsis is a fatal organ dysfunction caused by the host's dysregulated response to infection, emerging as the leading predisposing factor for acute kidney injury (AKI) in critically ill patients [1,2]. The onset of AKI significantly worsens the clinical outcomes of septic patients, incurring increased in-hospital mortality, length of hospital stays, and cost of care [3]. Unfortunately, there is a lack of specific pharmacological therapy that is effective enough for preventing or treating sepsis-induced AKI (SI-AKI), and severe cases generally resort to kidney replacement therapy as a supportive therapy [4]. Hence, more efforts should be conferred on clarifying the pathogenetic mechanism in order to develop effective intervention methods for patients with or predisposed to SI-AKI.

The septic environment is enriched with inflammatory mediatory molecules that trigger an inflammatory cascade,

leading to increased oxidative stress, with overproduction of reactive oxygen species (ROS), which disturb cellular energy metabolism by inducing mitochondria dysfunction [5]. Mitochondria are essential organelles that generate energy through oxidative phosphorylation (OXPHOS) in eukaryotic cells [6]. During sepsis, renal tubular epithelial cells (RTECs) undergo metabolic adaptation to downregulate aerobic glycolysis and upregulate OXPHOS, thereby reducing the host's predisposition to AKI [7–9]. However, the induction of mitochondria dysfunction by excessive ROS in RTECs gives rise to apoptosis of RTECs, thus contributing to AKI occurrence in septic patients [5,10].

Methylenetetrahydrofolate dehydrogenase 2 (MTHFD2) is a mitochondrial folate one-carbon (1C) enzyme with methylene dehydrogenase and cyclohydrolase activity [11], which catalyzes the mitochondrial reaction in 1C metabolism (also called the folate metabolic pathway), a metabolic process supporting

CONTACT Weike Hu  fyyhuweike@nbu.edu.cn  Department of Emergency Medicine, The First Affiliated Hospital of Ningbo University, No. 59 Liuting Street, Ningbo, Zhejiang Province 315010, China

© 2024 The Author(s). Published by Informa UK Limited, trading as Taylor & Francis Group
This is an Open Access article distributed under the terms of the Creative Commons Attribution-NonCommercial License (<http://creativecommons.org/licenses/by-nc/4.0/>), which permits unrestricted non-commercial use, distribution, and reproduction in any medium, provided the original work is properly cited. The terms on which this article has been published allow the posting of the Accepted Manuscript in a repository by the author(s) or with their consent.

various physiological processes, including nucleotide biosynthesis, amino acid homeostasis, S-adenosylmethionine production, and redox defense [12]. MTHFD2 has been proven to maintain active OXPHOS to ensure the integrity of the mitochondrial respiratory chain, thereby preventing mitochondrial dysfunction in mouse pluripotent stem cells [6]. Besides, from the dataset GSE60088, which demonstrates the gene expression pattern in septic kidney tissue, we identified an expression of MTHFD2. Accordingly, we speculated that MTHFD2 might be upregulated upon AKI as a protective action that relieves mitochondrial dysfunction to reduce RTEC injury in SI-AKI.

Histone acetylation represents the epigenetic machinery that loosens the condensed chromatin from its interaction with histone *via* histone acetyltransferases (HATs)-mediated acetylation of lysine residues of histone proteins to allow the access of activators or inhibitors of gene transcription, thereby modulating gene expression; this process can be reversed by histone deacetylases (HDACs), which remove acetyl groups from lysine residues of histone proteins [13]. HDACs assume a close association with the pathogenesis of AKI [14], while HATs exhibit dynamic alterations in their activities along the progression of AKI [15]. E1A binding protein p300 (EP300) is a HAT that induces acetylation of histone H3 lysine 27 (H3K27ac) [16], a marker indicative of active gene transcription [17]. Moreover, EP300 has been recognized as a core pivotal transcription factor for hub genes pertinent to the mechanism of AKI [18]. Through bioinformatics analysis, we were informed that EP300 can be enriched in the promoter region of MTHFD2. These findings together with the above speculation on MTHFD2 led to a conjecture that EP300 alleviated SI-AKI by facilitating H3K27ac to induce MTHFD2 upregulation and thus inhibit RTEC mitochondrial dysfunction.

In this current study, we used lipopolysaccharide (LPS)-induced RTECs to mimic *in-vitro* SI-AKI, whereby we investigated whether EP300 could alleviate SI-AKI by mediating H3 acetylation elevates MTHFD2 expression to inhibit mitochondrial dysfunction.

Methods and materials

Cell culture

The rat renal tubular epithelial NRK-52E cell lines were purchased from American Type Culture Collection (ATCC; CRL-1571, Manassas, VA, USA), and cultivated in Dulbecco's modified Eagle's medium (DMEM; 11965092, ThermoFisher, Waltham, MA, USA) plus 5% fetal bovine serum (F8687, Sigma-Aldrich, St. Louis, MO, USA) and 1% penicillin-streptomycin (TMS-AB2, Sigma-Aldrich, USA) at 37°C with 5% CO₂.

Exposure to LPS

NRK-52E cells were exposed to 0, 0.1, 0.5, and 1 µg/mL LPS (L5293, Sigma-Aldrich, USA) at 37°C for 24 h [19] and then the assessment of the expression of MTHFD2 in these cells was conducted, based on the results of which, the LPS

concentration optimum for the establishment of *in-vitro* SI-AKI models was determined to be 1 µg/mL. LPS at this concentration was used in the rest of the SI-AKI modeling-related experiments.

Western blot

Total protein was extracted from NRK-52E cells using RIPA buffer added with protease inhibitors (87785, ThermoFisher, USA). The protein concentration was determined using a BCA kit (A53227, ThermoFisher, USA). An equal amount of the protein was separated by SDS-PAGE gel (1615100, BIO-RAD, Hercules, CA, USA), and electrophoretically transferred onto polyvinylidene fluoride membranes (1620256, BIO-RAD, USA), after which the membranes were blocked using 5% skimmed milk for 1 h at room temperature. Primary antibodies for MTHFD2 (ab307428, 37 kDa, 1:1000, Abcam, Cambridge, UK), EP300 (ab259330, 264 kDa, 1:1000, Abcam, UK), and GAPDH (ab8245, 36 kDa, 1:1000, Abcam, UK) were utilized to incubate the membranes at 4°C overnight. After being washed by TBST (37573, ThermoFisher, USA) thrice, the membranes were further incubated with HRP-labeled secondary antibodies (Goat anti-Rabbit/Mouse IgG; ab97051/ab205719, Abcam, UK) at room temperature for 1 h. The protein signals were detected using ECL Substrate (1705060, BIO-RAD, USA) on an imaging system (ChemiDoc, BIO-RAD, USA), following which image analysis was performed using Image-Pro Plus (6.0 version, Media Cybernetics, Silver Spring, MD, USA).

For mitochondrial marker TOM20, mitochondria were prepared by cell mitochondria isolation kit (C3601, Beyotime, Shanghai, China). Cells (5×10^7) were harvested and washed with cold PBS. And cells were centrifuged at 4°C for 5 min, then discard the supernatant, and the precipitate was added 2 mL of mitochondrial separation reagent and placed in an ice bath for 10–15 min. The homogenate is then homogenized in a cold grinder, and the cell homogenate is then centrifuged at 4°C for 10 min. Carefully removed the supernatant and separated the precipitated cell mitochondria. Finally, mitochondrial were subjected to western blot. Primary antibody is TOM20 (ab186735, 16 kDa, 1:1000, Abcam, UK), and secondary antibodies is Goat anti-Rabbit IgG (ab97051, Abcam, UK), GAPDH (ab8245, 36 kDa, 1:1000, Abcam, UK) was the internal parameter of mitochondrial protein.

Cell transfection

Short hairpin RNA against MTHFD2 (shMTHFD2; TR707895) and overexpression plasmids for MTHFD2 (RR209354) were procured from OriGene (Rockville, MD, USA), while short hairpin RNA against EP300 was customized by GenePhrama (Suzhou, China). pCMV6-Entry vectors (NC; PS100001, OriGene, USA) and pRS vectors (shNC; TR20003, OriGene, USA) were used as the negative control for the overexpression plasmids and shRNA, respectively. NRK-52E cells were transfected with these plasmids alone or with NC plus

shEF300, MTHFD2 overexpression plasmids plus shNC, NC plus shNC or shEF300 plus MTHFD2 overexpression plasmids. The transfection was implemented using Lipofectamine 3000 transfection reagent (L3000015, ThermoFisher, USA). Briefly, NRK-52E cells (1×10^4) were seeded in 96-well plates per well and grown to reach an 80% confluency. Gene-lipid complexes were obtained by mixing the above plasmids (0.2 μ g) and Lipofectamine 3000 transfection reagent (0.3 μ L) with Opti-MEM medium (15 μ L) and P3000 reagent (0.4 μ L) at 37°C for 15 min, and then were used to incubate the cells. After 48 h of transfection, the transfection efficiency was assessed using quantitative reverse transcription-polymerase chain reaction (qRT-PCR). Thereafter, transfected NRK-52E cells were subjected to LPS exposure.

Chromatin immunoprecipitation (CHIP)

After LPS stimulation, transfected/nontransfected NRK-52E cells were crosslinked in 1% formaldehyde (F92120, ACMEC biochemical, Shanghai, China) for 10 min, which was quenched using 2.5 M glycine (N85370, ACMEC biochemical, China). Then, the cells (4×10^6) were lysed using RIPA Lysis Buffer and sonicated to generate DNA fragments of 200–1000 bp. The sonicated lysates were centrifugation at 10,000 \times g for 10 min at 4°C, and the obtained supernatant was pre-cleared for 3 h using 20 μ L 50% protein A-agarose beads (21348, ThermoFisher, USA), after which antibody for H3K27ac (PA5-85524, ThermoFisher, USA) was added to precipitate the cross-linked protein-DNA complexes overnight at 4°C. Normal Rabbit IgG (ab171870, Abcam, UK) was used as the negative control. Subsequently, incubation with 40 μ L 50% protein A-agarose beads was conducted at 4°C for 2 h. Later, the beads were harvested and eluted to obtain the protein-DNA complexes, which were de-crosslinked at 65°C overnight, and digested using 0.05 mg/mL Proteinase K (P274341, Aladdin, Shanghai, China) at 45°C for 2 h. Finally, the precipitated DNA was amplified through qPCR, with primers for the promoter of MTHFD2 (listed in Table 1).

Qrt-PCR

Total RNA from transfected/nontransfected NRK-52E cells was extracted using Trizol reagent (15596026, ThermoFisher, USA). Single-strand cDNA was generated from 800 to 1000 ng of the RNA by using reverse transcription kits (K1622, Yaanda Biotechnology, Beijing, China) according to the manufacturer's protocols. Sequentially, the cDNA was amplified using Eastep qPCR Master Mix (LS2062, Promega, Madison, WI, USA) and primers (listed in Table 1) on a PCR system

(LightCycler 96, Roche, Indianapolis, IN, USA). The cycling condition was set as follows: 95°C for 10 min, followed by 40 circles of 95°C for 15 s and 60°C for 1 min. Relative mRNA expression levels were calculated using the $2^{-\Delta\Delta Ct}$ method [20], with GAPDH used as the normalizer.

3-(4,5-Dimethylthiazol-2-yl)-2,5-diphenyltetrazolium bromide (MTT) assay

Transfected/nontransfected NRK-52E cells were seeded in 96-well plates at a density of 5×10^3 cells/well, and exposed to LPS as indicated above. 10 μ L of MTT Reagent (M6494, 5 mg/mL, ThermoFisher, USA) were added to each well before the cells were further incubated at 37°C for 4 h. Following the incubation, the cell supernatant was carefully aspirated out and 100 μ L of dimethyl sulphoxide (1211006, Sigma-Aldrich, USA) was employed to dissolve the generated formazan. Lastly, the absorbance was read at 570 nm using a microplate reader (EMax Plus, Molecular Devices, Sunnyvale, CA, USA).

Terminal deoxynucleotidyl transferase-mediated dUTP nick end labeling (TUNEL) staining

Apoptosis was determined using one-step TUNEL cell apoptosis detection kits (C1088, Beyotime, Shanghai, China). In short, after exposure to LPS, transfected/nontransfected NRK-52E cells (1×10^6) were fixed in 4% paraformaldehyde (CL10571, ChemeGEN, Shanghai, China) for 30 min, and subjected to 5-min permeabilization using 0.3% Triton X-100 (P0097, Beyotime, China). TUNEL working solution (50 μ L) prepared by TdT enzyme, fluorescent marker solution, and TUNEL detection solution was added into the cells, followed by cell incubation at 37°C for 1 h in the dark. The TUNEL-positive cells were observed using a confocal microscope (Axio Imager 2, Carl Zeiss, Oberkochen, Germany) under $\times 200$ magnification.

MitoSOX staining

MitoSOX Red Mitochondrial Superoxide Indicator (M36008, ThermoFisher, USA) was used to detect the changes of mitochondrial ROS levels. The cells were loaded in the dark for 10 min with MitoSOX Red, then washed twice with PBS. Then, 4',6-diamidino-2-phenylindole (DAPI, 62248, ThermoFisher, USA) were used to redye the cell. Fluorescent images were captured using a fluorescence microscope (Olympus BX 60, Olympus, Tokyo, Japan) and analyzed using Image J software (version 1.8.0, National Institutes of Health, Bethesda, MD, USA).

Table 1. Primers used in quantitative reverse transcription polymerase chain reaction for related genes.

Genes	Species	Forward (5'–3')	Reverse (5'–3')
MTHFD2	rats	TGACTGTCACACGAGCAGAC	GTCTTGAGGCACTGCAGAT
MTHFD2-promoter	rats	GCCAATCAGAACCTGCTCCT	CTCCTGAGCCGGCATAGAAG
EP300	rats	TTGGAACCTCAACTCGGGCTC	ACCAGGCAGAGGCAGATAGA
GAPDH	rats	TGGATAGGGTGGCCGAAGTA	TACAAGGGGAGCAACACGCTG

JC-1 staining

The mitochondrial membrane potential (MMP) was examined using JC-1 staining kits (C2003S, Beyotime, China). After exposure to LPS nontransfected/transfected NRK-52E cells were adjusted to a cell suspension with a concentration of 6×10^5 cells/mL. JC-1 staining solution (0.5 mL) was added to incubate the cells at 37°C for 20 min in the dark. Later, the fluorescence emitted by the aggregate JC-1 (red) and the monomer JC-1 (green) was observed using the confocal microscope under $\times 200$ magnification.

Statistical analysis

Data are expressed as mean \pm standard deviation of results derived from three different biological replications. Statistical analysis was achieved with Graphpad prism (version 8.0, GraphPad Software Inc., San Diego, CA, USA). Comparisons between two groups were conducted with independent *t*-tests, while those among multiple groups was undertaken with one-way analysis of variance (ANOVA). The difference was considered significant at $p < .05$.

Results

MTHFD2 was upregulated by LPS exposure and its overexpression antagonized LPS-induced apoptosis and mitochondrial dysfunction of NRK-52E cells

The mRNA expression of MTHFD2 was increased in a concentration-dependent manner by LPS (0.1, 0.5 and 1 μ g/mL) in NRK-52E cells (Figure 1A; $p < .05$). The protein expression level of MTHFD2 was observed to rise concentration-dependently in NRK-52E cells following exposure to LPS (0.1, 0.5 and 1 μ g/mL) (Figure 1B; $p < .05$). Subsequently, we manipulated MTHFD2 expression in NRK-52E cells through transfecting shMTHFD2 or MTHFD2 overexpression plasmids into cells and subjected the cells to LPS exposure to investigate the role of MTHFD2 in mitochondrial dysfunction elicited by SI-AKI. The results of transfection were shown in Figure 1C, E, which indicated that MTHFD2 was successfully knocked down or overexpressed by the corresponding plasmids in NRK-52E cells ($p < .001$). Then, the transfection efficiency was verified by western blot (Figure 1D,F; $p < .001$). MTT assay conducted to measure cell viability displayed that the viability of NRK-52E cells declined due to LPS exposure, and MTHFD2 knockdown further reduced the viability of LPS-exposed NRK-52E cells, while MTHFD2 overexpression alleviated the viability-reducing effect of LPS (Figure 1G; $p < .001$). Meanwhile, a drastically increased number of apoptotic NRK-52E cells positive for TUNEL was induced by LPS stimulation in NRK-52E cells (Figure 1H; $p < .001$). This LPS-induced apoptosis of NRK-52E cells intensified with MTHFD2 knockdown (Figure 1H; $p < .01$), but MTHFD2 overexpression repressed NRK-52E cell apoptosis induced by LPS (Figure 1H; $p < .05$).

Through mitoxox assay, LPS exposure was observed to cause accumulation of ROS in NRK-52E cells (Figure 2A,C;

$p < .001$). LPS-exposed NRK-52E cells undergoing MTHFD2 knockdown revealed a higher level of ROS than those without MTHFD2 knockdown (Figure 2A,C; $p < .001$). MTHFD2 overexpression resisted ROS accumulation caused by LPS stimulation in NRK-52E cells (Figure 2A,C; $p < .001$). Thereafter, JC-1 staining was performed to examine the collapse of MMP. As shown in Figure 2B,D, when being exposed to LPS, NRK-52E cells showed a shift of the aggregate JC-1 to the monomer JC-1, as evidence by a transition of the JC-1 fluorescence from red to green, which indicates a loss of MMP (Figure 2B,D). This LPS-induced MMP loss was potentiated by MTHFD2 knockdown, whereas being resisted after MTHFD2 overexpression (Figure 2B,D). Then, the expression of mitochondrial outer membrane marker TOM20 in LPS-exposed NRK-52E cells was detected by western blot, the result showed that MTHFD2 knockdown decreased the expression of TOM20 in the membrane, and overexpression MTHFD2 had the opposite effect (Figure 2E,F; $p < .01$). Overall, these data suggest that MTHFD2 expression may be a protective mechanism that is activated upon pathogenic stimulation to withstand mitochondrial dysfunction in SI-AKI.

EP300-mediated H3K27ac at the MTHFD2 promoter was essential to the antagonistic impact of MTHFD2 on LPS-induced apoptosis and mitochondrial dysfunction of NRK-52E cells

EP300 functions as a HAT which regulates transcription via chromatin remodeling [16]. The result of qRT-PCR and western blot showed that the expression of EP300 soared in NRK-52E cells owing to the LPS challenge (Figure 3A,B; $p < .001$). To ascertain whether EP300 has an implication in the effect of MTHFD2 to resist mitochondrial dysfunction caused by SI-AKI, ablation of EP300 was implemented. As shown in Figure 3C,D, EP300 was ablated by transfection with shEP300 in NRK-52E cells ($p < .001$). Moreover, EP300 ablation inhibited MTHFD2 expression (Figure 3E,F; $p < .001$). Then, through CHIP, we observed that LPS exposure augmented the H3K27ac antibody-mediated enrichment of the MTHFD2 promoter from NRK-52E cells, and transfection with EP300 silencing decreased LPS-caused effect (Figure 3G; $p < .001$), suggesting that LPS facilitates H3K27ac at the MTHFD2 promoter, which was reduced by EP300 ablation.

LPS-exposed NRK-52E cells exhibited reduced viability following EP300 ablation (Figure 3H; $p < .001$). The viability of LPS-exposed NRK-52E cells increased with MTHFD2 overexpression, which could be decreased by EP300 ablation (Figure 3H; $p < .01$). MTHFD2 overexpression revoked the viability reduction by EP300 ablation in LPS-exposed NRK-52E cells (Figure 3H; $p < .001$). In the presence of LPS, the number of TUNEL-positive apoptotic NRK-52E cells increased with EP300 ablation but decreased with MTHFD2 overexpression (Figure 4A,D; $p < .05$). Further, EP300 ablation and MTHFD2 overexpression antagonized each other's effect on the apoptosis of LPS-exposed NRK-52E cells (Figure 4A,D; $p < .01$). EP300 ablation resulted in ROS

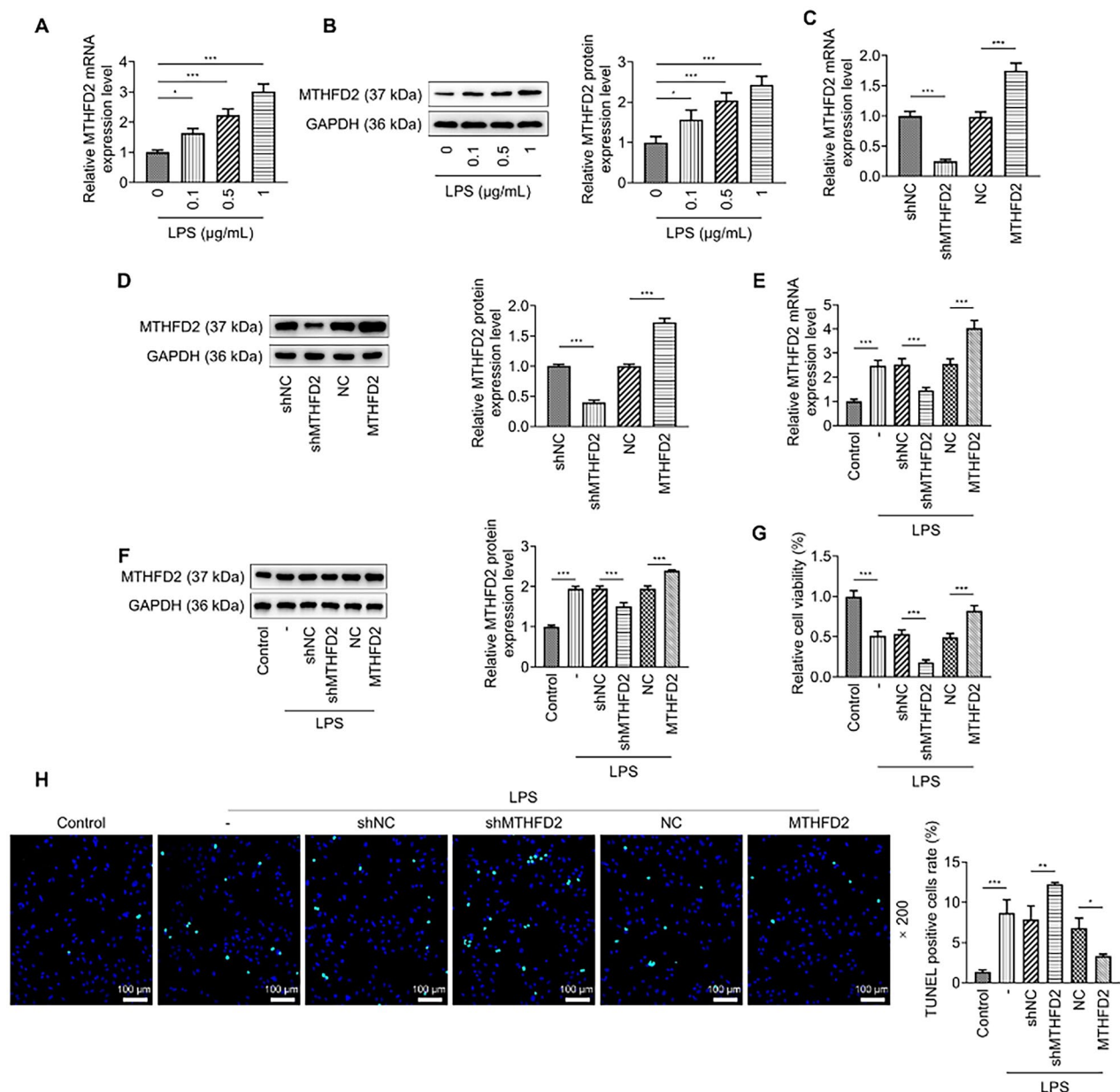


Figure 1. MTHFD2 was upregulated by LPS exposure and its overexpression antagonized LPS-induced apoptosis of NRK-52E cells. (A and B) The expression of MTHFD2 in NRK-52E cells that had received a 24-h exposure to 0, 0.1, 0.5 and 1 μg/mL LPS was analyzed by qRT-PCR and Western blot, with GAPDH serving as the normalizer. (C and D) The expression of MTHFD2 in NRK-52E cells transfected with shMTHFD2/shNC or MTHFD2 overexpression plasmids/NC was assessed by qRT-PCR and Western blot, with GAPDH serving as the normalizer. (E/F/G/H). NRK-52E cells were transfected with shMTHFD2/shNC or MTHFD2 overexpression plasmids/NC and exposed to 1 μg/mL LPS for 24 h. (E and F) The expression of MTHFD2 was assessed by qRT-PCR and Western blot, with GAPDH serving as the normalizer. (G). The viability of NRK-52E cells was measured by MTT assay. (H). The apoptosis of NRK-52E cells was checked using TUNEL staining (magnification, × 200; scale bar, 100 μm). * $p < .05$; ** $p < .01$; *** $p < .001$; *compares the values located at both ends of the line segment. LPS: lipopolysaccharide; MTHFD2: methylenetetrahydrofolate dehydrogenase 2; MTT: 3-(4,5-Dimethylthiazol-2-yl)-2,5-diphenyltetrazolium bromide; TUNEL: terminal deoxynucleotidyl transferase-mediated dUTP nick end labeling.

accumulation in LPS-stimulated NRK-52E cells, but ROS accumulation was mitigated when MTHFD2 was overexpressed in the cells (Figure 4B,E; $p < .01$). On the contrary, the MTHFD2 overexpression-mediated clearance of ROS in LPS-stimulated NRK-52E cells was abolished by EP300 ablation (Figure 4B,E; $p < .01$). LPS-exposed NRK-52E cells showed a transition of the JC-1 fluorescence from red to green due to EP300 ablation, representing a decreased MMP (Figure 4C,F; $p < .001$). Moreover, MTHFD2 overexpression increased the proportion of cells emitting red JC-1

fluorescence among LPS-exposed NRK-52E cells; besides, MTHFD2 overexpression reversed the effect of EP300 silencing (Figure 4C,F; $p < .01$). Moreover, EP300 silencing decreased the expression of TOM20 and MTHFD2 overexpression increased the expression of TOM20, however, MTHFD2 overexpression reversed the effect of EP300 (Figure 5A,B, $p < .001$). Taken together, these findings suggest that EP300-mediated histone acetylation is essential for MTHFD2 to exert antagonism toward mitochondrial dysfunction in SI-AKI.

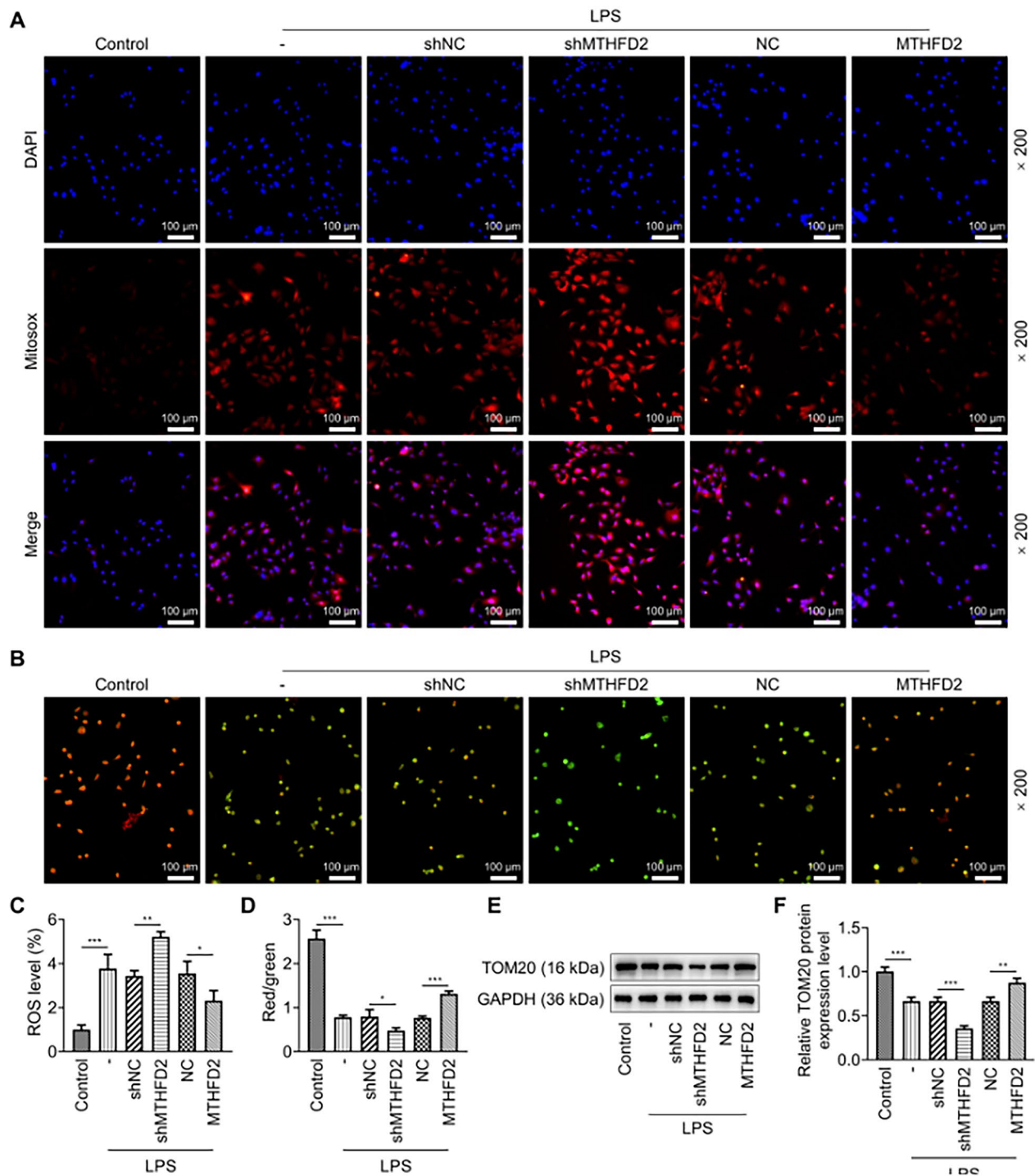


Figure 2. MTHFD2 was upregulated by LPS exposure and its overexpression antagonized mitochondrial dysfunction of NRK-52E cells. (A–F) NRK-52E cells were transfected with shMTHFD2/shNC or MTHFD2 overexpression plasmids/NC and exposed to 1 μ g/mL LPS for 24 h. (A and C) The level of ROS in NRK-52E cells was detected using mitosox assay (magnification, $\times 200$; scale bar, 100 μ m). (B and D) the mitochondrial membrane potential of NRK-52E cells was detected using JC-1 staining (magnification, $\times 200$; scale bar, 100 μ m). (E and F) the expression of TOM20 was detected by Western blot. * $p < .05$; ** $p < .01$; *** $p < .001$; *compares the values located at both ends of the line segment. LPS: lipopolysaccharide; MTHFD2: methylenetetrahydrofolate dehydrogenase 2; ROS: reactive oxygen species; DCFH-DA: 2',7'-dichlorodihydrofluorescein diacetate; qRT-PCR: quantitative reverse transcription-polymerase chain reaction; NC: negative control; shNC: short hairpin RNA against NC; shMTHFD2: short hairpin RNA against MTHFD2.

Discussion

SI-AKI is a common, life-threatening condition in critically ill, in-hospital patients [21]. Energy metabolism dysfunction

occurs in AKI and acts as a contributor to the disease pathogenesis [22]. Since mitochondria is the center of energy metabolism, delving into the mechanism underlying the dysfunction of mitochondria may lead to greater insights

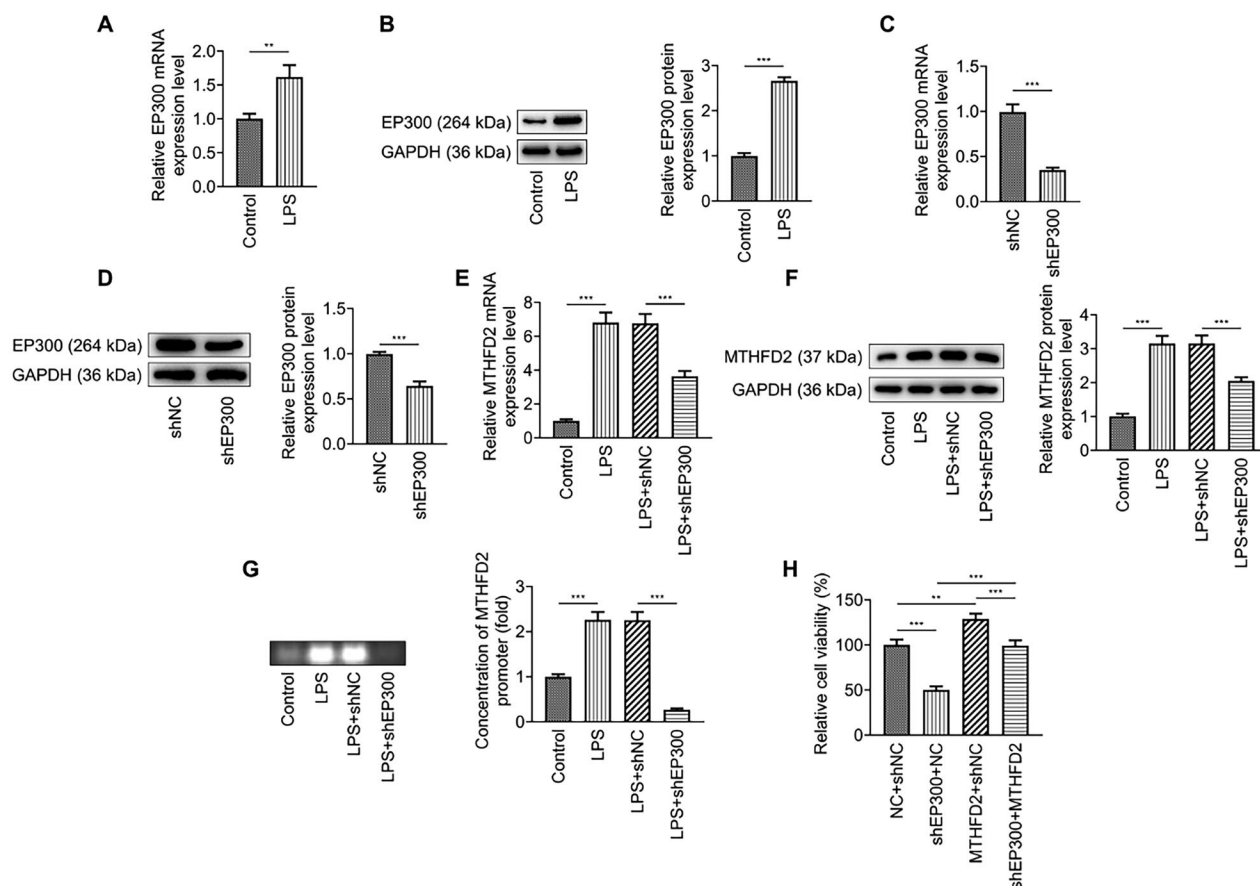


Figure 3. EP300-mediated H3K27ac at the MTHFD2 promoter was essential to the antagonistic impact of MTHFD2. (A and B) The expression of EP300 in NRK-52E cells that had received a 24-h exposure to 1 μ g/mL LPS was analyzed by qRT-PCR and Western blot, with GAPDH serving as the normalizer. (C and D) The expression of EP300 in NRK-52E cells transfected with shEP300/shNC was assessed by qRT-PCR and Western blot, with GAPDH serving as the normalizer. (E and F) In NRK-52E cells that had received a 24-h exposure to 1 μ g/mL LPS following transfection with EP300 overexpression plasmids/NC, the expression of MTHFD2 was detected by qRT-PCR and Western blot. (G) Whether EP300-mediated H3K27 acetylation occurs at the MTHFD2 promoter was determined using chromatin immunoprecipitation, in NRK-52E cells that had received a 24-h exposure to 1 μ g/mL LPS following transfection with EP300 overexpression plasmids/NC or not. (H) NRK-52E cells were transfected with NC plus shNC, shEP300 plus NC, MTHFD2 overexpression plasmids plus shNC or shEP300 plus MTHFD2 overexpression plasmids and exposed to 1 μ g/mL LPS for 24 h, the viability of NRK-52E cells was measured by MTT assay. ** $p < .01$; *** $p < .001$; *compares the values located at both ends of the line segment. LPS: lipopolysaccharide; MTHFD2: methylenetetrahydrofolate dehydrogenase 2; EP300: E1A binding protein p300; MTT: 3-(4,5-Dimethylthiazol-2-yl)-2,5-diphenyltetrazolium bromide; qRT-PCR: quantitative reverse transcription-polymerase chain reaction; NC: negative control; shNC: short hairpin RNA against NC; shEP300: short hairpin RNA against EP300.

into the pathogenesis of SI-AKI and point to a novel treatment for patients with SI-AKI.

MTHFD2 is a NAD-dependent, dehydrogenase and cyclohydrolase activity exhibiting, bifunctional metabolic enzyme, which participates in the catalysis of 1C metabolism of folate in mitochondria [23]. MTHFD2 is broadly expressed during embryogenesis, driving the folate metabolic pathway to produce nucleotide needed by cell proliferation, while showing extremely low or no expression in the majority of adult tissues as this pathway is activated at a basal level by a relatively low efficient enzyme, MTHFD2L [24,25]. Notably, in mouse pluripotent stem cells, MTHFD2 has been proven to prevent mitochondrial dysfunction by contributing to the integrity of the mitochondrial respiratory chain [6]. These above data hint that MTHFD2 has a mitochondrial protective role during embryogenesis but not in adulthood. Interestingly, the dataset GSE60088 reveals an expression of MTHFD2 in septic kidney tissue, and our study obtained a similar result in LPS-induced *in vitro* AKI. Since septic insults

cause ROS overproduction, which disrupts the quality control mechanisms of mitochondria, leading to mitochondrial dysfunction [26], the above findings and hint together elicit a question whether this MTHFD2 expression relieves SI-AKI-associated mitochondrial dysfunction in RTECs.

Mitochondrial dysfunction in kidney injury results in the generation of less energy, which can cause cell death, as a result of the unmet need of energy essential for cell function and survival [26]. Besides, fragmented mitochondria emerge due to excessive mitochondrial fission/fusion trigger by septic insults and release proapoptotic factors to the cytoplasm, inducing cell apoptosis [22]. During SI-AKI, RTECs exhibit significant apoptosis [27]. MTHFD2 has been reported to be anti-apoptotic in several types of cancer cells [28–30]. In LPS-induced NRK-52E cells, we observed a similar antiapoptotic role as well as a viability-restoring role of MTHFD2. These results contribute to the rationality of the notion that MTHFD2 expression protects RTECs against mitochondrial dysfunction in SI-AKI. Furthermore, mitochondria represent a

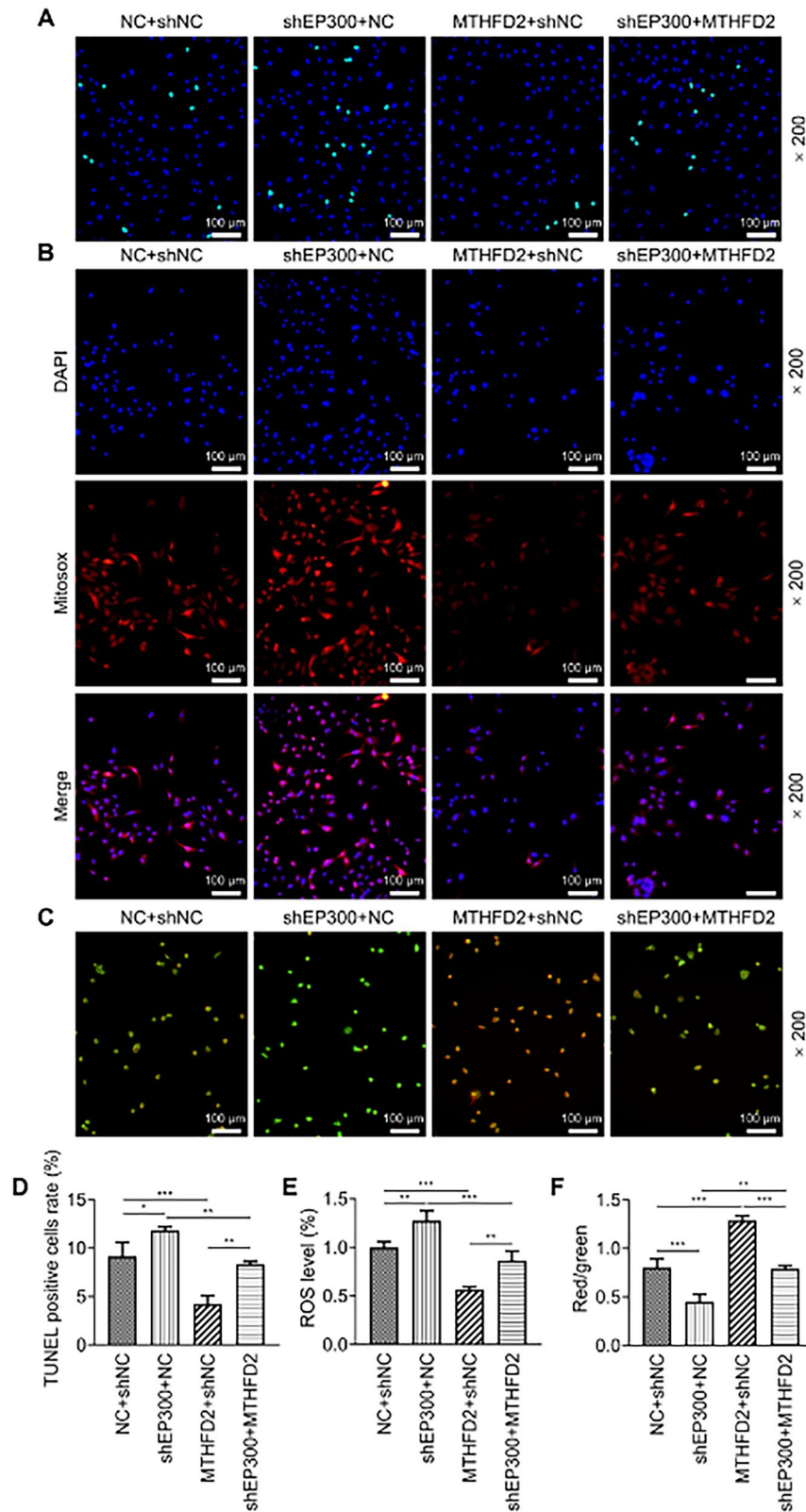


Figure 4. EP300-mediated H3K27ac at the MTHFD2 promoter was essential to the antagonistic impact of MTHFD2 on LPS-induced apoptosis and mitochondrial dysfunction of NRK-52E cells. (A–F). NRK-52E cells were transfected with NC plus shNC, shEP300 plus NC, MTHFD2 overexpression plasmids plus shNC or shEP300 plus MTHFD2 overexpression plasmids and exposed to 1 μg/mL LPS for 24 h. (A and D). The apoptosis of NRK-52E cells was checked using TUNEL staining (magnification, × 200; scale bar, 100 μm). (B and E). The level of ROS in NRK-52E cells was detected mitoxox assay (magnification, × 200; scale bar, 100 μm). (C and F). The mitochondrial membrane potential of NRK-52E cells was detected using JC-1 staining (magnification, × 200; scale bar, 100 μm). * $p < .05$, ** $p < .01$, *** $p < .001$; *compares the values located at both ends of the line segment. TUNEL: terminal deoxynucleotidyl transferase-mediated dUTP nick end labeling; ROS: reactive oxygen species; DCFH-DA: 2',7'-dichlorodihydrofluorescein diacetate; H3K27ac: acetylation of histone H3 lysine 27; qRT-PCR: quantitative reverse transcription-polymerase chain reaction; NC: negative control; shNC: short hairpin RNA against NC; shEP300: short hairpin RNA against EP300.

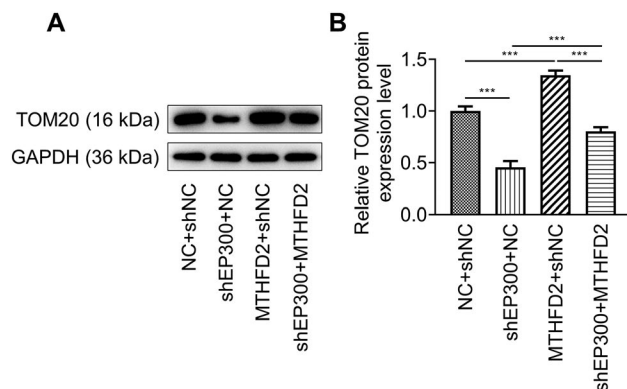


Figure 5. MTHFD2 overexpression reversed the decreased TOM20 expression by EP300 silencing. NRK-52E cells were transfected with NC plus shNC, shEP300 plus NC, MTHFD2 overexpression plasmids plus shNC or shEP300 plus MTHFD2 overexpression plasmids and exposed to 1 µg/mL LPS for 24 h. (A and B) The expression of TOM20 was detected by Western blot. *** $p < .001$; *compares the values located at both ends of the line segment.

major source of ROS in cells; upon mitochondrial damage, ROS accumulates [22], which results in the conversion of cytochrome c from an electron carrier into a peroxidase that oxidizes cardiolipin, leading to increased permeabilization of mitochondrial outer membranes; this further causes the release of mitochondrial ROS and cytochrome c to the cytoplasm, subsequently incurring proliferation inhibition and apoptosis induction [31,32]. Our data denoted that MTHFD2 expression negatively correlated with ROS accumulation and MMP collapse in LPS-induced NRK-52E cells, which justifies the above-mentioned notion. Besides, previous studies have shown that inhibiting sideroptosis of RTECs can improve sepsis induced acute kidney injury [33]. However, whether MTHFD2 suppress tubular ferroptosis induced by LPS is still need more experiments to identified.

Histone acetylation is a posttranslational modification that plays a part in the mechanism of AKI and changes in a time-and/or context (modeling approach)- dependent manner along the progression of AKI [15]. Histone acetylation is conferred by HATs but removed by HDACs [34]. In LPS-induced AKI/SI-AKI models, treatment with an inhibitor of HDAC1 and HDAC2 promoted H3 acetylation and reduced degree of renal injury [35], and administration of the selective class IIa HDAC elevated H3 acetylation, concomitant with mitigated renal tubular cell apoptosis and inflammation [36]; by contrast, increased acetylation of H3K18 acetylation favors the expressions of inflammatory genes [37]. EP300 functions as a HAT for H3K27 [16], and in our study, it was found to be upregulated in NRK-52E cells following LPS stimulation, suggesting that H3K27ac may impact the process of LPS-induced SI-AKI. HATs transfer an acetyl functional group to the lysine of core histones to acetylate histone, which weakens the histones and DNA interaction, rendering DNA more accessible to the transcription machinery and thus promoting gene transcription [38]. H3K27ac marks active gene transcription [17]. Our study showed that EP300 overexpression contributed to H3K27ac at the MTHFD2

promoter, suggesting that EP300-mediated H3K27ac at the MTHFD2 promoter acts as the upstream mechanism of MTHFD2 expression elevation in LPS-induced NRK-52E cells. EP300 has been proven to have essential roles in controlling cell growth and cell division [39] and to be required for mitochondrial biogenesis against renal ischemia/reperfusion injury [40], which combined with our results further suggest that EP300 may reduce RTEC mitochondrial dysfunction by upregulating MTHFD2 to protect RTECs during SI-AKI. This suggestion was later confirmed as rational by our results that revealed a MTHFD2 upregulation-dependent role of EP300 ablation to combat LPS-induced injury and mitochondrial dysfunction of NRK-52E cells.

However, there are some limitations in this study, first, our results demonstrate that MTHFD2 inhibits mitochondrial dysfunction under controlled conditions remains unknown, therefore, the detailed mechanism needs to be further studied. Second, whether EP300 knockout can block the expression of MTHFD2 without LPS treatment also needs to be further investigated. Moreover, this result has not been verified *in vivo* experiment, which is a limitation of our study, and we need to design more *in vivo* experiments to verified this in the future.

Conclusion

In conclusion, our *in-vitro* experiment data signified that LPS induced upregulation of EP300, which mediates H3K27ac at the MTHFD2 promoter to elevate MTHFD2 expression in NRK-52E cells as a protective mechanism against mitochondrial dysfunction. This finding provides a theoretical basis for the treatment of SI-AKI and also warrants a future study to verify whether our present results can be translated into animal models.

Disclosure statement

No potential conflict of interest was reported by the author(s).

Funding

This study was supported by Zhejiang Medicine and Health Science and Technology Project [2024KY1489].

Data availability statement

The datasets generated during and/or analyzed during the current study are available from the corresponding author on reasonable request.

References

- [1] Liu J, Xie H, Ye Z, et al. Rates, predictors, and mortality of sepsis-associated acute kidney injury: a systematic review and meta-analysis. *BMC Nephrol.* 2020;21(1):318. doi: 10.1186/s12882-020-01974-8.

- [2] Huang SJ, Ai T, Hu H, et al. Immunotherapy for sepsis induced by infections: clinical evidence and potential targets. *Discov Med.* 2022;34(172):83–95.
- [3] Poston JT, Koyner JL. Sepsis associated acute kidney injury. *BMJ.* 2019;364:k4891. doi: [10.1136/bmj.k4891](https://doi.org/10.1136/bmj.k4891).
- [4] Agapito Fonseca J, Gameiro J, Marques F, et al. Timing of initiation of renal replacement therapy in sepsis-associated acute kidney injury. *J Clin Med.* 2020;9(5):1413. doi: [10.3390/jcm9051413](https://doi.org/10.3390/jcm9051413).
- [5] Chang YM, Chou YT, Kan WC, et al. Sepsis and acute kidney injury: a review focusing on the bidirectional interplay. *Int J Mol Sci.* 2022;23(16):9159. doi: [10.3390/ijms23169159](https://doi.org/10.3390/ijms23169159).
- [6] Yue L, Pei Y, Zhong L, et al. Mthfd2 modulates mitochondrial function and DNA repair to maintain the pluripotency of mouse stem cells. *Stem Cell Reports.* 2020;15(2):529–545. doi: [10.1016/j.stemcr.2020.06.018](https://doi.org/10.1016/j.stemcr.2020.06.018).
- [7] Escobar DA, Botero-Quintero AM, Kautza BC, et al. Adenosine monophosphate-activated protein kinase activation protects against sepsis-induced organ injury and inflammation. *J Surg Res.* 2015;194(1):262–272. doi: [10.1016/j.jss.2014.10.009](https://doi.org/10.1016/j.jss.2014.10.009).
- [8] Yang L, Xie M, Yang M, et al. PKM2 regulates the Warburg effect and promotes HMGB1 release in sepsis. *Nat Commun.* 2014;5(1):4436. doi: [10.1038/ncomms5436](https://doi.org/10.1038/ncomms5436).
- [9] Opal SM, Ellis JL, Suri V, et al. Pharmacological SIRT1 activation improves mortality and markedly alters transcriptional profiles that accompany experimental sepsis. *Shock.* 2016;45(4):411–418. doi: [10.1097/SHK.0000000000000528](https://doi.org/10.1097/SHK.0000000000000528).
- [10] Guo J, Wang R, Liu D. Bone marrow-derived mesenchymal stem cells ameliorate sepsis-induced acute kidney injury by promoting mitophagy of renal tubular epithelial cells via the SIRT1/Parkin axis. *Front Endocrinol.* 2021;12:639165. doi: [10.3389/fendo.2021.639165](https://doi.org/10.3389/fendo.2021.639165).
- [11] Tibbetts AS, Appling DR. Compartmentalization of mammalian folate-mediated one-carbon metabolism. *Annu Rev Nutr.* 2010;30(1):57–81. doi: [10.1146/annurev.nutr.012809.104810](https://doi.org/10.1146/annurev.nutr.012809.104810).
- [12] Ducker GS, Rabinowitz JD. One-carbon metabolism in health and disease. *Cell Metab.* 2017;25(1):27–42. doi: [10.1016/j.cmet.2016.08.009](https://doi.org/10.1016/j.cmet.2016.08.009).
- [13] Tessarz P, Kouzarides T. Histone core modifications regulating nucleosome structure and dynamics. *Nat Rev Mol Cell Biol.* 2014;15(11):703–708. doi: [10.1038/nrm3890](https://doi.org/10.1038/nrm3890).
- [14] Hyndman KA. Histone deacetylases in kidney physiology and acute kidney injury. *Semin Nephrol.* 2020;40(2):138–147. doi: [10.1016/j.semnephrol.2020.01.005](https://doi.org/10.1016/j.semnephrol.2020.01.005).
- [15] Guo C, Dong G, Liang X, et al. Epigenetic regulation in AKI and kidney repair: mechanisms and therapeutic implications. *Nat Rev Nephrol.* 2019;15(4):220–239. doi: [10.1038/s41581-018-0103-6](https://doi.org/10.1038/s41581-018-0103-6).
- [16] Ogryzko VV, Schiltz RL, Russanova V, et al. The transcriptional coactivators p300 and CBP are histone acetyltransferases. *Cell.* 1996;87(5):953–959. doi: [10.1016/S0092-8674\(00\)82001-2](https://doi.org/10.1016/S0092-8674(00)82001-2).
- [17] Durbin AD, Wang T, Wimalasena VK, et al. EP300 selectively controls the enhancer landscape of MYCN-amplified neuroblastoma. *Cancer Discov.* 2022;12(3):730–751. doi: [10.1158/2159-8290.CD-21-0385](https://doi.org/10.1158/2159-8290.CD-21-0385).
- [18] Sun T, Cao Y, Huang T, et al. Comprehensive analysis of fifteen hub genes to identify a promising diagnostic model, regulated networks, and immune cell infiltration in acute kidney injury. *J Clin Lab Anal.* 2022;36(11):e24709. doi: [10.1002/jcla.24709](https://doi.org/10.1002/jcla.24709).
- [19] Wang L, Li J, Yu C. SENP3 aggravates renal tubular epithelial cell apoptosis in lipopolysaccharide-induced acute kidney injury via deSUMOylation of Drp1. *Kidney Dis.* 2022;8(5):424–435. doi: [10.1159/000525308](https://doi.org/10.1159/000525308).
- [20] Livak KJ, Schmittgen TD. Analysis of relative gene expression data using real-time quantitative PCR and the 2(-Delta Delta C(T)) Method. *Methods.* 2001;25(4):402–408.
- [21] Manrique-Caballero CL, Del Rio-Pertuz G, Gomez H. Sepsis-associated acute kidney injury. *Crit Care Clin.* 2021;37(2):279–301. doi: [10.1016/j.ccc.2020.11.010](https://doi.org/10.1016/j.ccc.2020.11.010).
- [22] Sun J, Zhang J, Tian J, et al. Mitochondria in sepsis-induced AKI. *J Am Soc Nephrol.* 2019;30(7):1151–1161. doi: [10.1681/ASN.2018111126](https://doi.org/10.1681/ASN.2018111126).
- [23] Christensen KE, Mirza IA, Berghuis AM, et al. Magnesium and phosphate ions enable NAD binding to methylenetetrahydrofolate dehydrogenase-methenyltetrahydrofolate cyclohydrolase. *J Biol Chem.* 2005;280(40):34316–34323. doi: [10.1074/jbc.M505210200](https://doi.org/10.1074/jbc.M505210200).
- [24] Nilsson R, Jain M, Madhusudhan N, et al. Metabolic enzyme expression highlights a key role for MTHFD2 and the mitochondrial folate pathway in cancer. *Nat Commun.* 2014;5(1):3128. doi: [10.1038/ncomms4128](https://doi.org/10.1038/ncomms4128).
- [25] Di Pietro E, Sirois J, Tremblay ML, et al. Mitochondrial NAD-dependent methylenetetrahydrofolate dehydrogenase-methenyltetrahydrofolate cyclohydrolase is essential for embryonic development. *Mol Cell Biol.* 2002;22(12):4158–4166. doi: [10.1128/MCB.22.12.4158-4166.2002](https://doi.org/10.1128/MCB.22.12.4158-4166.2002).
- [26] Tang C, Cai J, Yin XM, et al. Mitochondrial quality control in kidney injury and repair. *Nat Rev Nephrol.* 2021;17(5):299–318. doi: [10.1038/s41581-020-00369-0](https://doi.org/10.1038/s41581-020-00369-0).
- [27] Takasu O, Gaut JP, Watanabe E, et al. Mechanisms of cardiac and renal dysfunction in patients dying of sepsis. *Am J Respir Crit Care Med.* 2013;187(5):509–517. doi: [10.1164/rccm.201211-1983OC](https://doi.org/10.1164/rccm.201211-1983OC).
- [28] Yang S, Wong KH, Hua P, et al. ROS-responsive fluorinated polyethyleneimine vector to co-deliver shMTHFD2 and shGPX4 plasmids induces ferroptosis and apoptosis for cancer therapy. *Acta Biomater.* 2022;140:492–505. doi: [10.1016/j.actbio.2021.11.042](https://doi.org/10.1016/j.actbio.2021.11.042).
- [29] Wu S, Cai W, Shi Z, et al. Knockdown of MTHFD2 inhibits proliferation and migration of nasopharyngeal carcinoma cells through the ERK signaling pathway. *Biochem Biophys Res Commun.* 2022;614:47–55. doi: [10.1016/j.bbrc.2022.05.007](https://doi.org/10.1016/j.bbrc.2022.05.007).
- [30] Li Q, Yang F, Shi X, et al. MTHFD2 promotes ovarian cancer growth and metastasis via activation of the STAT3 signaling pathway. *FEBS Open Bio.* 2021;11(10):2845–2857. doi: [10.1002/2211-5463.13249](https://doi.org/10.1002/2211-5463.13249).
- [31] Birk AV, Chao WM, Bracken C, et al. Targeting mitochondrial cardiolipin and the cytochrome c/cardiolipin complex to promote electron transport and optimize mitochondrial ATP synthesis. *Br J Pharmacol.* 2014;171(8):2017–2028. doi: [10.1111/bph.12468](https://doi.org/10.1111/bph.12468).
- [32] Wan J, Kalpage HA, Vaishnav A, et al. Regulation of respiration and apoptosis by Cytochrome c threonine 58 phosphorylation. *Sci Rep.* 2019;9(1):15815. doi: [10.1038/s41598-019-52101-z](https://doi.org/10.1038/s41598-019-52101-z).
- [33] Guo J, Wang R, Min F. Ginsenoside Rg1 ameliorates sepsis-induced acute kidney injury by inhibiting ferroptosis in renal tubular epithelial cells. *J Leukoc Biol.* 2022;112(5):1065–1077. doi: [10.1002/JLB.1A0422-211R](https://doi.org/10.1002/JLB.1A0422-211R).

- [34] Wang J, Shen F, Liu F, et al. Histone modifications in acute kidney injury. *Kidney Dis.* 2022;8(6):466–477. doi: [10.1159/000527799](https://doi.org/10.1159/000527799).
- [35] Cheng S, Wu T, Li Y, et al. Romidepsin (FK228) in a mouse model of lipopolysaccharide-induced acute kidney injury is associated with down-regulation of the CYP2E1 gene. *Med Sci Monit.* 2020;26:e918528. doi: [10.12659/MSM.918528](https://doi.org/10.12659/MSM.918528).
- [36] Zhang W, Guan Y, Bayliss G, et al. Class IIa HDAC inhibitor TMP195 alleviates lipopolysaccharide-induced acute kidney injury. *Am J Physiol Renal Physiol.* 2020;319(6):F1015–f1026. doi: [10.1152/ajprenal.00405.2020](https://doi.org/10.1152/ajprenal.00405.2020).
- [37] Huang J, Wan D, Li J, et al. Histone acetyltransferase PCAF regulates inflammatory molecules in the development of renal injury. *Epigenetics.* 2015;10(1):62–72. doi: [10.4161/15592294.2014.990780](https://doi.org/10.4161/15592294.2014.990780).
- [38] Shen F, Zhuang S. Histone acetylation and modifiers in renal fibrosis. *Front Pharmacol.* 2022;13:760308. doi: [10.3389/fphar.2022.760308](https://doi.org/10.3389/fphar.2022.760308).
- [39] Liang W, Yamahara K, Hernando-Erhard C, et al. A reciprocal regulation of spermidine and autophagy in podocytes maintains the filtration barrier. *Kidney Int.* 2020;98(6):1434–1448. doi: [10.1016/j.kint.2020.06.016](https://doi.org/10.1016/j.kint.2020.06.016).
- [40] Wang D, Wang Y, Zou X, et al. FOXO1 inhibition prevents renal ischemia-reperfusion injury via cAMP-response element binding protein/PPAR- γ coactivator-1 α -mediated mitochondrial biogenesis. *Br J Pharmacol.* 2020;177(2):432–448. doi: [10.1111/bph.14878](https://doi.org/10.1111/bph.14878).